Water vapor retrieval in the upper troposphere and lower stratosphere using airborne measurements of spectral solar irradiance

Peter Stammer*, Kevin Wolf, André Ehrlich, Manfred Wendisch

*Institut of Meteorology, Stephanstr. 3 04103 Leipzig, *E-Mail: p.stammer@hotmail.com*

Summary

Airborne measurements of the downward spectral solar irradiance were analyzed with differential optical absorption spectroscopy for the integrated water vapor (IWV) in the atmospheric column above the aircraft. The measurements are obtained from two campaigns in 2016, during which the High Altitude and Long Range Research Aircraft (HALO) took measurements of the downward solar irradiance within the upper troposphere and lower stratosphere (UTLS). The feasibility and limitations of the presented method are discussed for the dry conditions, which are typical for the high altitudes of the UTLS and above. Considering the uncertainties encountered in the irradiance measurements and the high sensitivity of the retrieval, the method was unable to provide sound results for the stratosphere, but provided reasonable results in the troposphere.

Zusammenfassung

Flugzeuggetragene Messungen der abwärtsgerichteten spektralen solaren Irradianz wurden mit der Methode der differenziellen optischen Absorptionsspektroskopie auf den integrierten Wasserdampf (IWV) in der Atmosphäre oberhalb des Flugzeuges untersucht. Im Rahmen zweier Messkampagnen im Jahr 2016 führte das High Altitude and Long Range Research Aircraft (HALO) Messungen der spektralen solaren Irradianz in dem Höhenbereich der oberen Troposphäre und unteren Stratosphäre (UTLS) durch. Hier werden das Potential und die Limitierungen eines solchen Verfahrens untersucht, um Wasserdampf in den trockenen Gegebenheiten abzuleiten, die in und oberhalb der UTLS herrschen. Angesichts der Messunsicherheiten und der hohen Sensitivität des Verfahrens, konnten in der Statosphäre nicht aussagekräftige Ergebnisse erreicht werden, aber in der Troposphäre konnte das Verfahren zuverlässige Ergebnisse liefern.

1 Motivation

The amount of water vapor in the upper troposphere and lower stratosphere (UTLS) is significantly lower, compared to tropospheric water vapor, but it has significant impacts on radiative and dynamical processes (Maycock et al., 2013) and therefore influences the earth's climate (Solomon et al., 2010). Additionally, water vapor has an impact on the troposphere-stratosphere exchange and serves as a tracer for investigating the stratosphere (Fueglistaler et al., 2009).

Longterm records of water vapor in the UTLS are scarce in number and often have low temporal or spatial coverage. Measurements of water vapor in high altitudes by in situ observations is challenging due to the low concentrations in the dry stratosphere. There is evidence for a gradual increase of stratospheric water vapor over the past decades, but the responsible processes are not completely understood (Hurst et al., 2011).

Remote sensing by measurements of downward solar radiation were already used by Houghton and Seeley (1960) to quantify the integrated water vapor at high altitudes over England. This water vapor remote sensing generally relies on the principle of differential optical absorption spectroscopy (DOAS). Kindel et al. (2015) discussed an example of the application of DOAS for retrieving water vapor both within a constrained layer in the atmosphere, as well as within the atmospheric column above an aircraft up to the top of the atmosphere (TOA). Their study concluded that the airborne measurements have the ability to probe the mechanisms of stratospheric water vapor transport at a higher vertical and horizontal resolution and higher accuracies than would be possible with balloon or satellite measurements.

In the study presented here, this method was adapted to spectral solar irradiance measurements obtained on board of the research aircraft HALO (High Altitude and Long Range Research Aircraft), which are described in Section 3. In Section 2, the retrieval method is described and characterized by a sensitivity study. Exemplary results are presented in Sections 4-5.

2 Differential optical absorption spectroscopy

2.1 Theory

The retrieval of water vapor by means of differential optical absorption spectroscopy (DOAS) relies on the absorption of solar radiation by atmospheric water vapor. Solar radiation that is incident on the top of the atmosphere (TOA) has an initial spectral irradiance $F_{\lambda,0}$. After propagating through the atmosphere by a certain path length s, the irradiance is reduced to $F_\lambda(s)$ by absorption by water vapor, as described by Lambert-Beer's,

$$F_\lambda(s) = F_{\lambda,0} \cdot exp\left(-\frac{\tau}{\mu}\right) = F_{\lambda,0} \cdot exp\left(-b_{abs}\frac{z}{\mu}\right) = F_{\lambda,0} \cdot exp\left(k \cdot \rho_{wv}\frac{z}{\mu}\right) = F_{\lambda,0} \cdot exp\left(k\frac{IWV}{\mu}\right), \tag{1}$$

when considering the geometry $s = z/\mu$ and $\mu = cos\theta$ being defined as the cosine of the solar zenith angle θ. In equation 1 the optical thickness τ equals the product s and the absorption coefficient b_{abs}. b_{abs} is equal to the product of the mass absorption coefficient k (m^2 kg^{-1}) of water vapor and the absolute humidity ρ_{wv}. ρ_{wv} integrated over s results in the integrated water vapor (IWV), which has the units kg m^{-2}.

Based on equation 1 the IWV can be derived by the ratio between the irradiance at TOA and at the irradiance at z, at a wavelength λ_{wv} where water vapor absorbs radiation. The strongest water vapor absorption bands in the visible range are centered at 0.82, 0.94 and 1.1 μm. The near-infrared (NIR) has absorption bands centered at 1.37, 1.87 and 2.6 μm. At the higher altitudes of concern for this work the NIR bands are no longer saturated, but are still strong enough that radiation is absorbed sufficiently despite the low IWV amounts. Therefore, the bands at 1.37 and 1.87 μm are both used to infer IWV in the UTLS.

F_0 cannot be measured directly, but is estimated instead by measurements at wavelengths near the water vapor absorption where there is no absorption by water vapor. There are many more processes besides the absorption by the trace gas that contribute to an extinction of radiation, such as Rayleigh scattering or effects in the measuring instrument (Platt and Stutz, 2008). Differential optical absorption spectroscopy solves this problem by observing the difference in the occurring absorption at several wavelengths. While absorption by the trace gas water vapor, the differential absorption, occurs over a narrow band, the rest of the factors that cause extinction generally have spectrally broad structures. The narrow band trace gas absorption can be separated from the broadband extinction. Therefore, broadband extinction is subtracted from F_0, and the resulting $F_0^{'}$ becomes the new intensity spectra of reference, to which the trace gas absorption is compared.

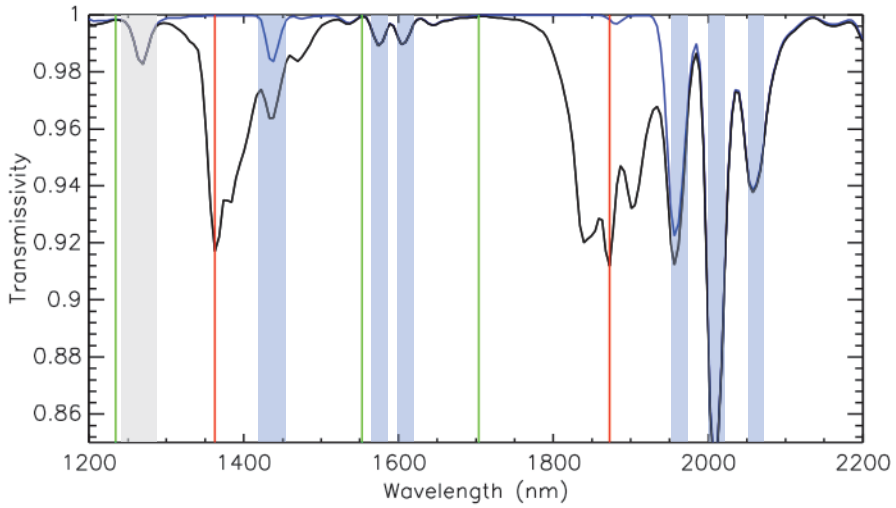

Fig. 1: *Spectral transmissivity of the US standard atmosphere as simulated at an altitude of 10 km for an atmosphere with water vapor (blue line) and without water vapor (black line). Red lines denote center of the two water vapor absorption bands in the NIR (1363 nm and 1873 nm) and the green lines denote minima in water vapor absorption (1235 nm, 1553 nm and 1704 nm) which can be used for scaling because they are close to the respective absorption band. The gray shaded region denotes absorption from O_2, the blue shaded region that of CO_2.*

Figure 1 gives a detailed picture of the water vapor absorption in the NIR. The blue line is the simulated transmittance of a model atmosphere considering all atmospheric gases besides water vapor, while the black line includes water vapor. In the regions where both lines differ, absorption by water vapor is involved. At the centers of both absorption bands, located at 1363 nm and 1873 nm (red lines), practically all molecular absorption is due to water vapor. The green lines denote examples of wavelengths that are close to the bands, at which the atmosphere is practically free of molecular absorption not only from water vapor but from all gases. These are 1235 nm, 1553 nm and 1704 nm.

One of these absorption-free wavelengths is used to scale the spectral irradiance to obtain $F_0^{'}$. Scaling is performed by means of a simple gain of the measurement across all wavelengths, so that the measured irradiance is identical to the TOA irradiance at the scaling wavelength. Performing such a scaling introduces relative irradiances instead of absolute irradiances. The quantity under consideration is now the relative relation between the band center and the scaling wavelength.

2.2 Iterative Retrieval

The downward spectral irradiance is simulated with the version 2.0.2 of the radiative transfer routines libRadtran (Emde et al., 2016). Calculation of radiative transfer in libRadtran is based primarily on the DISORT (DIScrete ORdinate Radiative Transfer solver) code. Simulations are performed for identical conditions for all relevant quantities, being the solar zenith angle, the flight altitude and atmospheric profiles above the aircraft. The simulated irradiance is then compared with the measurement.

The unknown quantity in the simulation is the IWV of the overlying atmospheric column. LibRadtran incorporates several model atmospheres that include, among other quantities, a profile of air temperature and water vapor. Model atmospheres are available for a range of latitudes and seasonal conditions. A profile is chosen according to the setting of the measurement. A custom model atmosphere is created be eliminating water vapor at all levels below the flight altitude. When adjusting the IWV of the simulation, the water vapor profile of the rest of the model atmosphere is scaled to the new IWV value while its shape is maintained.

The IWV is varied so that the simulated irradiance and the scaled measured irradiance within the water vapor absorption band match. Due to scaling both spectra at the wavelength outside the absorption band, this is the same as bringing the relative difference of the irradiance inside and outside the absorption band to unity. The retrieval of water vapor is performed by iteratively adjusting the input IWV of the model. With the measured irradiance $F_{meas}(\lambda_{wv})$ and the simulated irradiance $F_{sim}(\lambda_{wv}, IWV_n)$ the iteration is performed by:

$$IWV_{n+1} = \frac{F_{sim}(\lambda_{wl})}{F_{meas}(\lambda_{wl})} \cdot IWV_n \tag{2}$$

After a sufficiently large amount of iterations the iteration factor becomes close to one and the IWV converges. In the algorithm the iteration was stopped when the difference between the measured and the simulated water vapor absorption was minimized to below a certain threshold. This threshold was set to 0.01 % of the scaled measured irradiance.

2.3 Feasibility of retrieval method

The differences of transmissivity within and outside the water vapor absorption band become lower the higher measurement is made in the atmosphere and the less water vapor is above the aircraft. Therefore, the accuracy of the irradiance measurements needs to be sufficiently high in order to allow a reliable retrieval of IWV. Figure 2 shows the simulated spectral transmissivity at two altitudes (10 km and 15 km) in the model US standard atmosphere. The tropopause in this model atmosphere

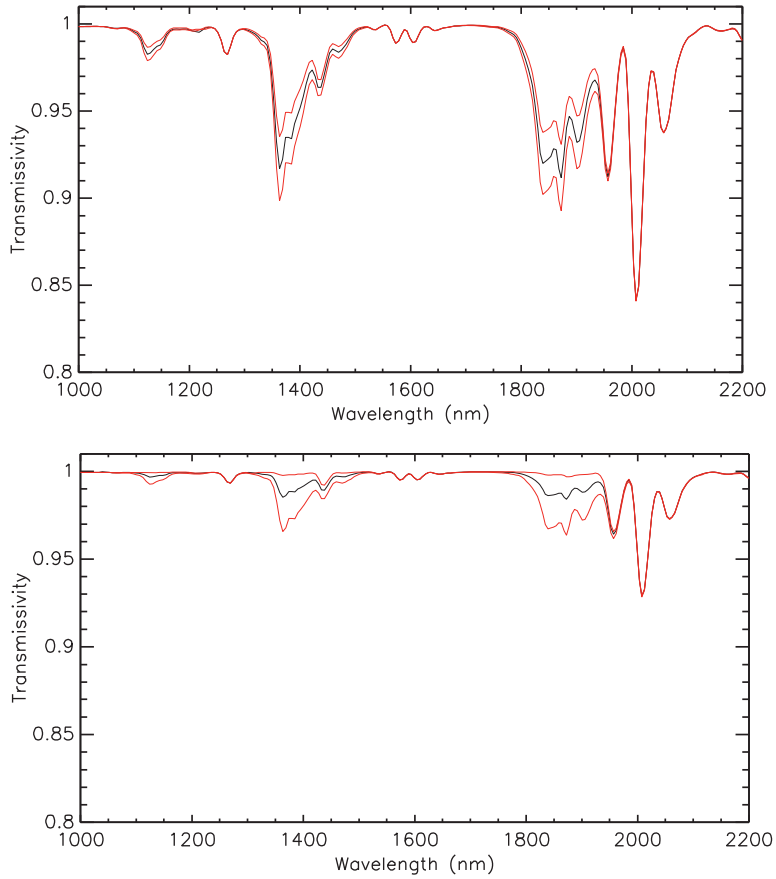

Fig. 2: *Spectral transmissivity (black line) of model US standard atmosphere at 10 km (top) and 15 km (bottom) and with the introduction a measurement uncertainty in the irradiance measurement of ±2% (red lines).*

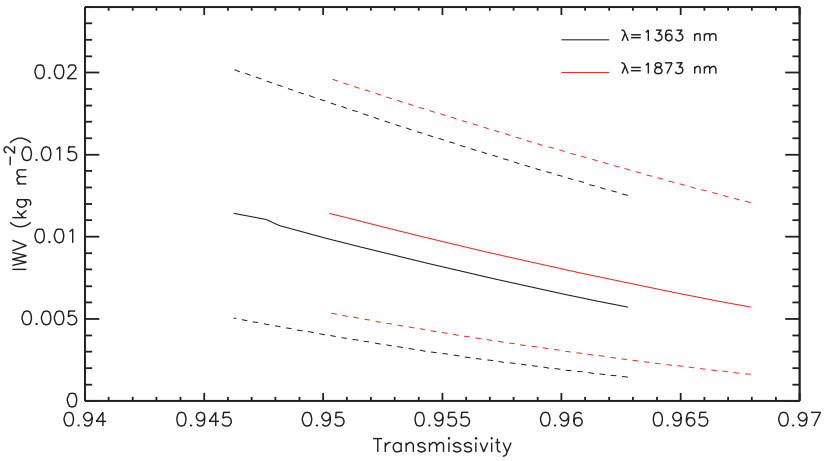

Fig. 3: *Retrieved IWV in dependance of the simulated transmissivity of the atmospheric column from 10 km altitude to the TOA. Dashed lines illustrate the +/-2 % uncertainty of SMART.*

is located at 11 km. There is a large difference in the strength of the water vapor absorption bands between both altitudes. An uncertainty for the measured irradiance of ± 2 % is a good first estimate. The effect of this uncertainty is considered by applying the ± 2 % uncertainty to the original irradiance (as represented by the black plots) and then applying the IWV retrieval to these modified irradiance spectra to deduce modified values for the IWV. These modified values for the IWV then produce new irradiance spectra, that are displayed as the red plots, thus representing the effective uncertainty of the IWV retrieval. The model atmosphere has an IWV of 0.031 mm at 10 km and 0.004 mm at 15 km. At 10 km the IWV uncertainty results in a clear spread within the water vapor absorption bands. At 15 km the IWV is so low that the upper bound in the irradiance measurement leads to a transmissivity spectrum in which water vapor absorption becomes vanishingly small.

In the next scenario a range of IWV values was created with an upper and lower bound, which were oriented towards the values of the stratospheric water vapor found by Hurst et al. (2011). These were 3.0 pmmv and 6.0 pmmv. For this range it was assumed that the water vapor mixing ratio between 10 km and the TOA was constant. Accordingly a range of transmittances in the water vapor bands were simulated at 10 km. Figure 3 displays the retrieved IWV as a function of detected transmissivity at 1363 nm and 1873 nm. The dashed lines display the respective range of the transmission due to the irradiance uncertainty. The change in transmissions over this range of IWV is quite small and would require a precise measurement for the concerning range of stratospheric water vapor. In comparison, uncertainty of the transmission is about as large as the actual variability of IWV. As the transmission is generally high for these low values of IWV even an uncertainty of 2 % for the absolute irradiance causes a large uncertainty in transmissivity. The resulting uncertainty of IWV is very large, between ± 50 % and ± 100 %.

Both the absolute and the relative uncertainty of the IWV retrieval vary, depending on the actual amount of IWV. The absolute uncertainty increases and the relative uncertainty decreases the higher the actual IWV is. The simulations from figure 2 result in an uncertainty of the IWV of +0.008 / -0.011 mm or +27 / -37 % at 10 km and +0.014 / -0.004 or +380 / -100 % on the upper bound at 15 km. When performing calculations in this way and assuming a 2 % uncertainty in the irradiance measurement we find that, in order to obtain an uncertainty of at most 5 % in the IWV one needs an IWV of at least around 1 kg m^{-2}. For comparison, this is the IWV one finds in the US standard atmosphere at an altitude of approximately 6 km. When assuming a spectrometer uncertainty of 0.1 %, as Kindel et al. (2015) applied, an uncertainty of 5 % can be achieved for an IWV as low as 0.05 kg m^{-2}, or at approximately 10 km altitude in the US standard atmosphere.

3 Measurement with HALO

The High Altitude and Long Range Research Aircraft (HALO) is a modified business jet that has been operated as a German research aircraft since 2009. HALO has some advantageous characteristics compared to other research aircraft, having a large payload, long flight ranges and durations and a high flight ceiling. The aircraft's maximum flight altitude is 15 km. Depending on the latitude, HALO can thus reach far into the stratosphere and is well suited for studying the UTLS.

In the past, HALO has carried several instruments that are capable of measuring low water vapor concentrations in the UTLS. In-situ measurements include the Fast In-Situ Stratospheric Hygrometer (FISH) and the Hygrometer for Atmospheric Investigation (HAI) (Rolf et al., 2015). HALO accommodates two nadir looking remote sensing instruments, which are the HALO Microwave Package (HAMP) and the WAter vapor Lidar Experiment in Space (WALES). Details on the instruments can be found in Schnitt et al. (2017) and Grooß et al. (2014). Being a microwave radiometer, HAMP infers the IWV of the column below the aircraft. The lidar instrument WALES infers a vertical profile of the water vapor mixing ratio.

The Next-generation Aircraft Remote-sensing for VALidation studies (NARVAL-II) and the North Atlantic Waveguide and Downstream impact EXperiment (NAWDEX) were two campaigns, that HALO performed in 2016. NARVAL-II took place from June 20 - August 31 and was located near Barbados. NAWDEX took place shortly afterwards from September 12 - October 16. This campaign was focused on the North Atlantic and was based on Iceland. The general cruise altitude during both campaigns was above 8 km and up to approximately 14 to 15 km. With both of these campaigns, measurements are available from the sub-tropics and midlatitude region. Depending on the geographical location the flight ceiling was in the upper troposphere or lower stratosphere.

3.1 Irradiance measurements on HALO

The Spectral Modular Airborne Measurement System (SMART)-Albedometer installed on HALO measures the spectral upward and downward solar irradiance with two optical inlets. These inlets are mounted to the upper and lower fuselage. A third inlet with a narrow field of view measures the upward radiance. The optical inlets are each connected with two grating photodiode array spectrometers by optical fibers. After entering into the spectrometer through a slit, the incoming radiation is spectrally dispersed by a reflective grating and is detected by an array of photo-diodes. Each diode measures a pixel in the spectrum. For a single scan of the spectrum the diodes count photons over an integrated measurement time of 0.5 s. The second spectrometer covers 950-2200 nm with 256 pixels. A description of SMART can by found e.g. in Bierwirth et al. (2009) and Ehrlich et al. (2008).

Another key component of the SMART-Albedometer is an active horizontal stabilization system, which reduces measurement uncertainty from misalignment of the sensors. For proper measurements of $F_\lambda^\downarrow$ the sensor must be aligned with the horizontal plane. Even small deviations from a horizontal alignment can cause significant measurement errors. Even during horizontal flight conditions it is impossible for the airplane to maintain a perfectly stable horizontal position and not experience variability of the pitch or roll angle. With a firm installation of the sensor to the aircraft fuselage an accuracy of ± 5 % or better would not be possible (Wendisch et al., 2001).

In order to solve this problem Wendisch et al. (2001) developed the active stabilization system, which maintains a horizontal alignment of the optical inlets during flight with respect to the earth-fixed coordinate system. A measurement unit determines the aircraft's changes in attitude using an artificial horizon, which it cross-checks with data from a global positioning system (GPS). The measured changes in attitude are then simultaneously compensated by an active horizontal adjustment system. With the active stabilization an accuracy of the sensor's horizontal alignment of better than

$\pm 0.2^\circ$ for pitch and roll angles of up to $\pm 6^\circ$ is obtained. For the measured irradiance the stabilization system thereby ensures an accuracy of better than ± 1 % (Wendisch et al., 2001).

Several components go into the measurement uncertainty of the irradiance. The photodiodes in the spectrometer give off electronic noise, the dark current, by producing a signal even when there is no incoming radiation. The instrument undergoes an absolute calibration in the laboratory for the pixel-wavelength assignment and the absolute irradiance. The spectrometer also undergoes a transfer calibration when it is moved into the field. These three components add to a total measurement uncertainty in the NIR between 8.3 % and 9.4 % (Brückner et al., 2014). The largest fraction of the total uncertainty is on account of the total calibration. When considering the ratio of the irradiance at two different wavelengths, as opposed to the absolute irradiance, the uncertainty of the spectrometer and transfer calibration can be ignored and only the uncertainty of the spectrometer signal remains relevant. Thus the uncertainty in the NIR is reduced to that of the spectrometer noise, with 1.8 % to 2.2 % (Brückner et al., 2014).

3.2 Water vapor retrieval

In theory the retrieval of the IWV is a straightforward process of matching the simulated and measured irradiances at the center of the absorption band. One of several technical limitations is the finite spectral resolution of the measurement. Each of the spectrometer's photodiodes is centered at a specific wavelength. The diode receives radiation not only from the infinitesimal spectral range of this wavelength, but from within a certain spectral interval that lies symmetrically around the center wavelength. Simulated spectra have an arbitrary resolution and consist of infinit points. In order to apply simulations to the measurements, the simulations need to be convoluted with a spectral slit function. This slit function is applied to each point of the simulated irradiance spectrum. It is essentially a Gaussian function with a full width at half maximum (FWHM) that matches that of the measurements pixel.

The FWHM varies throughout the spectrum and between the 1.4 μm and the 1.9 μm band. Choosing an accurate value for the FWHM becomes a trade-off between reproducing the center of an absorption band the most accurately or reproducing an absorption band as a whole the most accurately. The retrieval was performed for a suitable NAWDEX measurement made at 8 km using a range of values for the FWHM. The ideal value for the FWHM was determined from a combination of reducing the standard deviation in the difference between measured and simulated irradiance in the absorption band on the one hand and on the other hand a simple estimation by eyesight.

As the spectrometer has a limited resolution, it must be taken into account, that the spectrometer has no pixel that is centered at the precise location of the absorption band center and instead measures at wavelengths that are close to the center. Choosing the center of the absorption band becomes ambiguous. When looking at the 1363 nm absorption band, one notices a steep drop in absorption when moving along the spectrum away from the maximum. As a result, varying the wavelength in the retrieval slightly can result in differing values of the detected IWV. With that it becomes less clear how to interpret a simulation and a measurement that achieve identical absorption at a central wavelength of one of the absorption bands. Missing the theoretical center of the absorption band with the spectrometer has an effect on the quality of the retrieval. For the 1.4 μm band the center pixel of the measurement is at 1365 nm. Variation of the retrieval wavelength by the two adjacent pixels leads to a variation in retrieved IWV with a standard deviation of $5.5 \cdot 10^{-3}$ mm or approximately 7% of the retrieved IWV. In the case of the 1.9 μm the center pixel is at 1873 nm and variation has a standard deviation of $3 \cdot 10^{-3}$ mm or approximately 5% of the retrieved IWV. The retrieval is relatively sensitive to the FWHM of the slit function. A was to quantify this sensitivity is to observe the degree to which the retrieved IWV changes after changing the FWHM by a small value ($dIWV/dFWHM$.) For the

retrieval at 1365 nm the sensitivity is 0.003 mm/nm or approximately 3 % of the retrieved IWV and at 1873 nm this is 0.0044 mm/nm or 6 %.

A retrieval criteria that seems to be less sensitive to the measurement's finite resolution is to instead use the integral over a broader span of the water vapor absorption band. It would theoretically make sense to detect IWV by the entire spectral range of the absorption band. However, including the wings of the bands, where the water vapor signal becomes smaller, would also allow the noise in the measurement to obtain a greater influence. The integral range chosen for this work was from 1300 nm to 1500 nm for the 1.4 μm absorption band and 1750 nm to 1950 nm for the 1.9 μm absorption band. This is respectively approximately the entire span of the band. In comparing both retrieval methods, the integral method is less sensitive to the slit function. This is understandable, as the integration results in an averaging of the gap between measurement and simulation. The sensitivity $dIWV/dFWHM$ is 0.00019 mm/nm or 0.2 % for the 1.4 μm band and 0.00037 mm/nm or 0.5 % for the 1.9 μm band.

The retrieved values for IWV tend to be lower when retrieving with the 1900 nm band than with the 1400 nm band, both for the integral and for the wavelength method. On average the disagreement between both retrieval bands is smaller for the wavelength method than the integral method. The average deviation of the retrieved IWV between both wavelengths is 0.007 mm throughout the FWHM range of 10.8 - 15.6 nm for integral method versus 0.014 mm for the wavelength method.

The FWHM for the integral retrieval method was set to 15.6 nm for the 1.4 μm band and 10.8 for the 1.9 μm band. For the wavelength method the FWHM was 18.0 nm and 10.8 nm, respectively. With these slit functions the disagreement becomes twice as good for the integral method compared to the wavelength method. The disagreement for the central wavelength makes up 36 % of the mean IWV from both bands versus 19 % for the integral method. In the following the retrieval method of integration of the 1.4 μm band between 1.3 μm and 1.5 μm will be used. This method is less dependent on the FWHM of the slit function being applied to the simulation and shows fairly good agreement between both bands. Also, one can expect the 1.4 μm band to have a better signal-to-noise ratio than the 1.9 μm band, because the solar irradiance under a cloudless sky is stronger at a shorter wavelength within the NIR.

When evaluating a measured irradiance spectrum, first a moving average over three measurement pixels is applied to the measurement. This smooths out some of the high frequency structure in the signal caused by electronic noise and may decrease the uncertainty from pixel registration (Kaufman and Gao, 1992). Scaling of the measurement to the simulation is performed at 1553 nm for the 1.4 μm band or 1704 nm at the 1.9 μm band.

4 Estimation of Retrieval Uncertainty

The uncertainty in the IWV retrieval results from several factors. One of these is the uncertainty concerning the temperature and water vapor profile above the aircraft. Factors from the irradiance measurement itself include the uncertainty of the horizontal alignment of the optical inlets, as well as noise from the spectrometer. Noise sources, as stated by Platt and Stutz (2008) are photon statistics, electronic detector noise in the instrument and further, unexplained, random spectral structures in the signal. A reason for the latter factor can for example be pixel-to-pixel variations in sensitivity.

From the above section the uncertainty of the spectrometer irradiance amounts to ± 2 %. The active stabilization amounts to an uncertainty of ± 1 %. The latter is a conservative estimate and may actually be reduced further because it is the ratio of two irradiances from the same scan being considered for the retrieval and not an absolute irradiance.

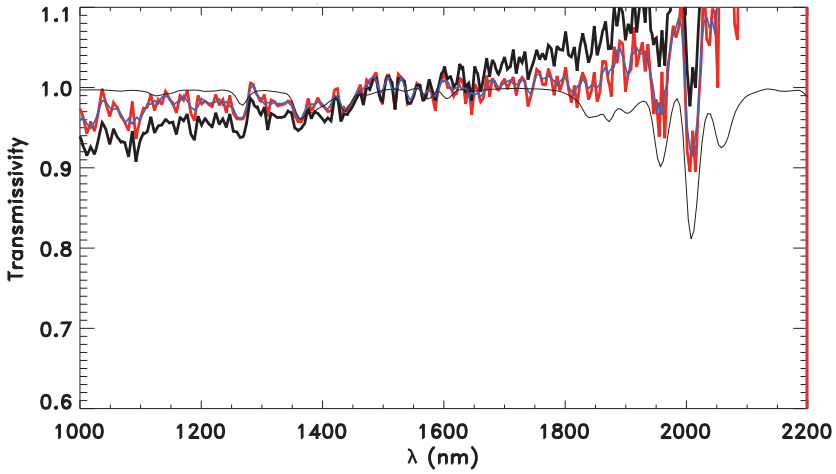

Fig. 4: *Spectral transmissivity measured at 12.3 km during a NAWDEX flight (red) and the spectral transmissivity averaged over 600 spectra (black). The blue plot is the result of a moving average over three pixels of the red plot.*

4.1 Spectral noise

Kindel et al. (2015) achieve an uncertainty for the spectrometer of only 0.1 % after averaging over 5 to 10 minutes of scans, or 300-600 spectra. For the measurements that were available for this work such a reduction in uncertainty was not achieved. The red plot in figure 4 shows an example of the spectral transmissivity from a single measurement taken during a cruise episode at 12.3 km during a NAWDEX flight. After averaging irradiance spectra over five minutes or approximately 600 spectra (black plot) the signal noise remains as high and shows a similar structure as the non-averaged spectrum. There must be a noise component that is due to spectral structures of the instrument.

Figure 5 shows the transmissivity from two scans taken at different altitudes during the NAWDEX campaign. Both spectra are now smoothed with the moving average. The signal noise was investigated using the standard deviation of the dispersion of the measured (red plot) from the theoretical irradiance as given by the simulation (black plot) in the range 1530 to 1700 nm. In this range water vapor has no influence. After applying the running average the standard deviation is reduced from $\sim$2 % to $\sim$1 %. The error bars denote the resulting water vapor uncertainty due to the signal noise.

In the case of the low measurement, where there is a strong water vapor signal, noise uncertainty results in a relative uncertainty in the IWV detection of 10%. For the high measurement this uncertainty in the order of 100 %. This confirms the apparent insight from the plot, which is that at a certain altitude the expected amount of water vapor becomes so low, that the resulting absorption signal becomes too weak to reliably detect.

4.2 Resulting total uncertainty in IWV retrieval

The total uncertainty of the relative irradiance is $\pm$3 %. The resulting uncertainty in the IWV retrieval is obtained by adjusting the measurement by $\pm$3 % and observing the resulting change in retrieved IWV. The absolute and the relative uncertainty of IWV are both not generally constant, but vary with the actual value of IWV. The calculated retrieval uncertainty is generally not symmetrical, which is in line with the physics of Lambert-Beer's law.

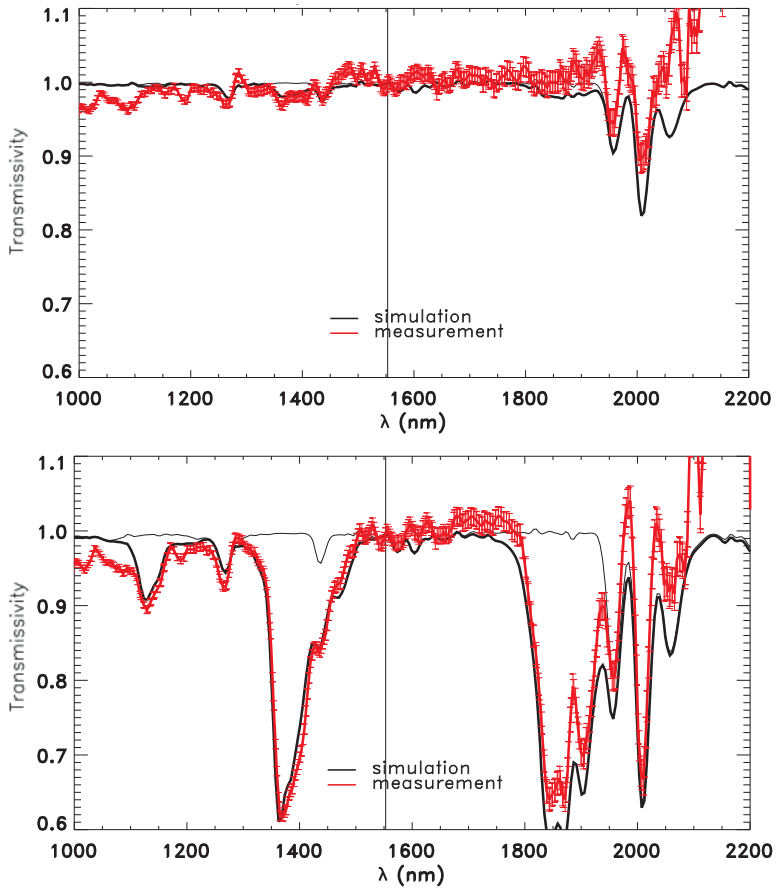

Fig. 5: *Spectral transmissivity measured at 12 km (left) and 7 km (right) and retrieved transmissivity with noise. Vertical line denotes scaling wavelength.*

For the measurement at 7 km from the bottom panel in figure 5 the calculated uncertainty is +0.059/-0.069 kg m^{-2} or +32/-38 %. This measurement was geographically in the North Atlantic and the flight altitude was thus roughly at the tropopause. At 12 km during the same flight the uncertainties grow to +0.049/-0.038 kg m^{-2} or +188/-92 %. This finding underlines the difficulty of the task at hand, because even small uncertainties of the irradiance lead to a large uncertainty in retrieved IWV due to the scarcity in water vapor that one encounters in the UTLS.

5 Results

NAWDEX measurements taken during a cruise segment at 12.3 km on the August 19 show a water vapor signal that is too low compared to the noise to deduce IWV. A model atmosphere for similar conditions (sub-arctic, summer) contains an IWV of 0.006 kg m^{-2} at this altitude. The uncertainty of the retrieval was calculated at +200/-100 %.

Figure 6 shows the time series of the retrieved IWV during a cruise at 9.7 km altitude on the September 21 during NARVAL-II. This is well below the tropopause and in a generally more moist atmosphere. The uncertainty here is +40/-34 %. The model atmosphere for the tropics has an IWV of 0.12 kg m^{-2}.

Another interesting consideration is to construct a vertical profile of the water vapor mixing ration or to retrieve the IWV for a limited layer of the atmosphere from measurements taken during ascent or descent of the aircraft. From the SMART measurements taken during the ascent on the same day

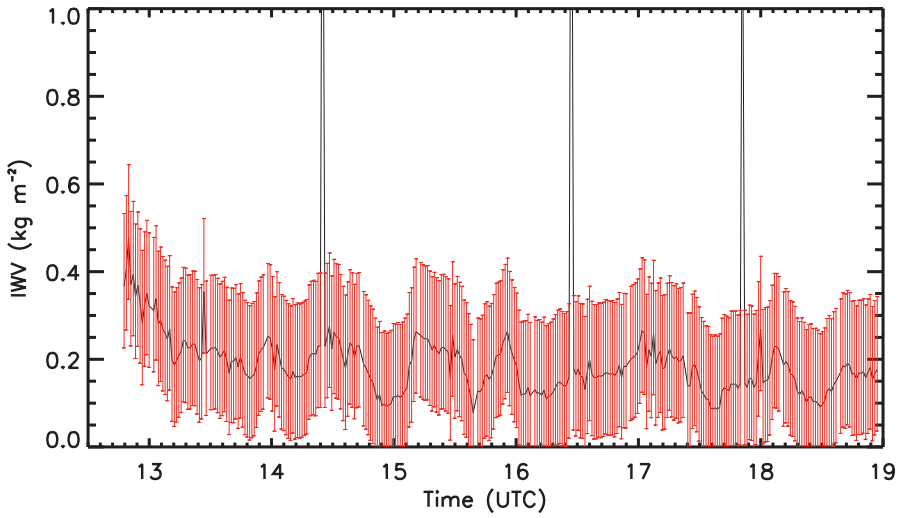

Fig. 6: *Time series of retrieved IWV during cruise at 9.7 km during a NARVAL-II flight with error bars (8:30 to 15:00 local time).*

the retrieved IWV in the layer between 4 km and 9.7 km is 2.43 +0.32/-0.36 kg m^{-2}. This can be compared to 3.21 kg m^{-2} from in-situ measurements of water vapor made on HALO and 2.74 kg m^{-2} from a radio sonde launched at the airport of take-off.

6 Conclusion

A DOAS method for retrieving the IWV from airborne measurements of the spectral solar irradiance has been introduced. The method relies on the water vapor absorption bands located at 1.37 μm and 1.87 μm in the NIR. The potential of thus retrieving the IWV near the UTLS has been analyzed. A sensitivity study showed that, as there is only a weak water vapor signal under such conditions, uncertainties in the radiation measurement lead to a large uncertainty in the retrieval. At 10 km the US standard atmosphere has an IWV of 0.03 kg m^{-2}. When applying an uncertainty of $\pm$2% for the irradiance measurement the resulting uncertainty of the retrieval was found to be +27/-37 %. In order to obtain a retrieval with an uncertainty of better than 5% the highest altitude for performing the retrieval would be 6 km. If, e.g, the uncertainty of the irradiance measurement could be decreased to only 0.1% the retrieval could perform with the same degree of certainty at altitudes of up to 10 km. The water vapor signal in HALO measurements taken in the stratosphere becomes indistinguishable above the signal noise and the stabilization uncertainty. Consideration of these data was limited to lower altitudes. As an example, a time series was created of the IWV at 9.7 km at the Bahamas. The retrieval uncertainty here was +40/-34 %. Also, from the aircraft's ascent after take-off, the IWV was retrieved within a layer between 4 and 9.7 km. The resulting value (2.43 +0.32/-0.36 kg m^{-2}) compared well with onboard in-situ and radiosonde measurements.

References

Bierwirth, E., Wendisch, M., Ehrlich, A., Heese, B., Tesche, M., Althausen, D., Schladitz, A., Müller, D., Otto, S., Trautman, T., Dinter, T., Hoyningen-Huene, W., Kahn, R., 2009: Spectral surface albedo over Morocco and its impact on radiative forcing of Saharan dust, Tellus, 61B, 252-269.

Brückner, M., B. Pospichal, A. Macke, M. Wendisch, 2014: A new multispectral cloud retrieval method for ship-based solar transmissivity measurements, J. Geophys. Res. Atmos., 119, 11,338-11,354.

Ehrlich, A., Bierwirth, E., Wendisch, M., Gayet, J.-F., Mioche, G., Lampert, A., Heintzenberg, J., 2008: Cloud phase identification of Arctic boundary-layer clouds from airborne spectral reflection measurements: test of three approaches, Atmos. Chem. Phys., 8, 7493-7505.

Emde, C., Buras-Schnell, R., Kylling, A., Mayer, B., Gasteiger, J., Hamann, U., Kylling, J., Richter, B., Pause, C., Dowling, T., Bugliaro, L., 2016: The libRadtran software package for radiative transfer calculations (version 2.0.1), Geosci. Model Dev., 9, 1647-1672.

Fueglistaler, S., Dessler, A. E., Dunkerton, T. J., Folkins, I., Fu, Q., Mote, P. W., 2009: Tropical Tropopause Layer, Rev. Geophys., 47, RG1004.

Groß, S., Wirth, M., Schäfler, A., Fix, A., Kaufmann, S., Voigt, C., 2014: Potential of airborne lidar measurements for cirrus cloud studies, Atmos. Meas. Tech., 7, 2745-2755.

Houghton, J. T., Seeley, J. S., 1960: Spectroscopic observations of the water-vapor content of the stratosphere, Quart. J. R. Met. Soc., 86, 358.

Hurst, D. F., Oltmans, S. J., Vömel, H., Rosenlof, K. H., Davis, S. M., Ray, E. R., Hall, E. G., Jordan, A. F., 2011: Stratospheric water vapor trends over Boulder, Colorado: Analysis of the 30 year Boulder record, J. Geophys. Res., 116, D02306.

Kaufman, Y. J., Gao, B.-C., 1992: Remote sensing of water vapor in the near IR from EOS/MODIS, IEEE TGRS, 30, 5.

Kindel, B. C., Pilewskie, P., Schmidt, K. S., Thornberry, T., Rollins, A., Bui, T., 2015: Upper-troposphere and lower-stratosphere water vapor retrievals from the 1400 and 1900 nm water vapor bands, Atmos. Meas. Tech., 8, 1147-1156.

Maycock, A. C., Joshi, M. M., Shine, K. P., Scaife, A. A., 2013: The Circulation Response to Idealized Changes in Stratospheric Water Vapor, Am. Met. Soc., 554-561.

Platt, U., Stutz, J., 2008: Differential Optical Absorption Spectroscopy: Principles and Applications, Springer-Verlag Berlin Heidelberg, p. 138 ff.

Rolf, C., Afchine, A., Bozem, H., Buchholz, B., Ebert, V., Guggenmoser, T., Hoor, P., Konopka, P., Kretschmer, E., Müller, S., Schlager, H., Spelten, N., Sumińska-Ebersoldt, O., Ungermann, J., Zahn, A., Krämer, M., 2015: Transport of Antarctic stratospheric strongly dehydrated air into the troposphere observed during the HALO-ESMVal campaign 2012, Atmos. Chem. Phys., 15, 9143-9158.

Schnitt, S., Orlandi, E., Mech, M., Ehrlich, A., Crewell, S., 2017: Characterization of Water Vapor and Clouds During the Next-Generation Aircraft Remote Sensing for Validation (NARVAL) South Studies, J-STARS, VOL. 10, NO. 7.

Solomon, S., Rosenlof, K. H., Portmann, R. W., Daniel, J. S., Davis, S. M., Sanford, T. J., Plattner, G.-K., 2010: Contributions of stratospheric water vapor changes to decadal variation in the rate of global warming, Science, 327, 1219-1223.

Wendisch, M., Müller, D., Schell, D., Heintzenberg, J., 2001: An airborne spectral albedometer with active horizontal stabilization. J. Atmos. Oceanic Technol.,18, 1856-1866.